



# Eco-friendly approach to mineralise 2-nitroaniline using subcritical water oxidation method: use of ANN and RSM in the optimisation and modeling of the process

Erdal Yabalak<sup>1</sup> · Özgür Yilmaz<sup>1</sup>

Received: 18 June 2018 / Accepted: 29 August 2018 / Published online: 1 September 2018  
© Iranian Chemical Society 2018

## Abstract

In this study, the mineralisation of 2-nitroaniline was investigated using the eco-friendly subcritical water oxidation method and the effective oxidising agent, H<sub>2</sub>O<sub>2</sub>. Central composite design was utilized to examine the effect of temperature, oxidant concentration, and treatment time on the mineralisation of 2-nitroaniline, to optimise the experimental process and to propose a theoretical equation of the chemical oxygen demand removal percentage. ANOVA test was performed to evaluate the reliability of the process. *F* and *p* values were obtained as 23.03 and < 0.0001, respectively. *R*<sup>2</sup> and adjusted *R*<sup>2</sup> were obtained as 0.9540 and 0.9126, respectively. Artificial neural network modeling was used to determine the predicted values. The efficiency of central composite design and artificial neural network was statistically compared as well as by closeness of their predicted values to the experimental values. The maximum chemical oxygen demand removal percentages of 2-nitroaniline at 473 K of temperature, 30 min of treatment time, and 30 mM of H<sub>2</sub>O<sub>2</sub> concentration were found to be 80.15 and 78.03% according to the predicted results of central composite design and artificial neural network. Removal of 2-nitroaniline was also followed using UV–Vis, FT-IR, and NMR spectroscopy. 2-Nitroaniline was removed by 99.88% at 473 K of temperature, 90 min of treatment time, and 120 mM of H<sub>2</sub>O<sub>2</sub>. Mineralisation and removal of 2-nitroaniline were also supported by FT-IR and NMR analyses.

**Keywords** 2-Nitroaniline · Mineralisation · Subcritical water · Artificial neural network · Response surface methodology

## Introduction

In recent years, water pollution caused by industrial wastes is known to be an increasing problem [1–5]. The identification of toxic hazardous compounds in such wastes and the removal of them from water sources is particularly a scientific and environmental problem. It is known that one of the most important molecular groups that cause water pollution are nitroaromatic compounds [6]. This compound and its derivatives are used as an intermediate in the production of

paint, agrochemicals, and some important polymers, as well as in the explosive and the pharmaceutical industry due to containing the nitro group [7–12]. Therefore, the nitroaromatic compounds, which are formed by the wastes generated in the above-mentioned industrial processes, seriously pollute soil and water resources.

In fact, the environmental contamination caused by nitroaromatic compounds occurs due to their ability to be readily reduced to carcinogenic amine derivatives [10, 13]. In addition, azo dyes in wastewater are known to undergo variations into highly toxic aromatic amine groups such as nitroaniline under anaerobic conditions. In particular, 2-nitroaniline (2-NA) and 4-nitroaniline compounds, which are well-known industrial pollutants due to their high stability and solubility, occupy the blood, liver, and central nervous system via the respiratory and digestive system and cause serious side effects on humans [14–17]. In addition, these nitroaniline compounds are used directly as intermediates in the production phase in many industrial fields [18, 19]. Therefore, nitroaromatics and nitroanilines are at the top

**Electronic supplementary material** The online version of this article (<https://doi.org/10.1007/s13738-018-1487-8>) contains supplementary material, which is available to authorized users.

✉ Erdal Yabalak  
yabalakerdal@gmail.com

<sup>1</sup> Department of Chemistry, Faculty of Arts and Science, Mersin University, Çiftlikköy Campus, 33343 Mersin, Turkey

of the priority pollutants of the list of United States Environmental Protection Agency for which removal processes need to be improved [10, 11]. Essentially, 4-nitroaniline has been reported by National Environmental Protection Agency of China as one of the prior pollutants to be removed from water sources [20, 21].

Although several methods were applied for the removal of nitroaniline compounds [22–27], they cannot effectively deal with resistant compounds such as nitroaniline and its derivatives. Furthermore, the effectiveness of biological processes remains limited in the treatment of resistant contaminants such as *p*-nitroaniline [28]. Thus, it can be said based on all these limitations that new, efficient, and environmentally friendly methods are still in great demand. Herein, we propose a solution for the over mentioned issues via degrading 2-NA by subcritical water oxidation (SWO) method in the presence of H<sub>2</sub>O<sub>2</sub>.

SWO is an environmentally friendly method besides defined as a process in which hydroxyl radicals and active oxygen species are thermochemically formed by taking the advantage of subcritical water [29, 30]. Subcritical water, which is provided by applying pressure to water heated between 373 and 647 K to keep it in liquid form, provides an unrivaled medium for degradation processes [31, 32]. The combined effect of subcritical water and innocuous oxidising agent, H<sub>2</sub>O<sub>2</sub>, offers favorable conditions for degradation of target molecules [30]. SWO has been proven to be a very effective method in the degradation of hazardous pollutants [32–36]. Another feature of this method, which is superior to conventional methods, is the short treatment time, which is an important parameter for process cost. Thus, it is clear that this performed method is an appropriate alternative to other methods in many respects.

In addition, response surface methodology (RSM) was utilized in this work to avoid waste of time, solvent, and cost [37]. Central Composite Design (CCD), which is one the several effective types of experimental design techniques of RSM, [32, 38, 39], was applied to optimise the experimental design. Furthermore, artificial neural network (ANN), which has been widely used and is an alternative modeling technique to RSM system [40, 41], was employed to model and optimise the experimental design. The basic advantage of ANN for being an alternative to RSM system is based on the ability of ANN to establish a non-linear relationship between the response and independent variables without any prior knowledge of the nature of this relationship [40–42]. The efficiency of CCD and ANN models in the estimation of the response was also statistically compared and both of the models were evaluated by their prediction capabilities over the coefficient of determination,  $R^2$ , the root mean square error (RMSE), and the absolute average deviation (AAD) values.

We aimed to mineralise 2-NA in aqueous solution, which represents a model for water contaminated by

2-NA, using SWO in the presence of H<sub>2</sub>O<sub>2</sub>. In this sense, the degradation rates were defined as removal percentage of chemical oxygen demand (COD) of treated samples. Furthermore, the removal of 2-NA was observed by UV–Vis, FT-IR, and NMR analyses. CCD was used to evaluate optimum experimental parameters of temperature, oxidising agent, and treatment time and their interactions on the response. Obtained predicted values, which were obtained by CCD and ANN models, were compared, and the efficiency of the models was statistically discussed.

## Experimental

### Reagents and apparatus

2-NA and H<sub>2</sub>O<sub>2</sub> were purchased from Sigma–Aldrich (St. Louis, MO). Ethyl acetate and Na<sub>2</sub>SO<sub>4</sub> were purchased from Merck (Darmstadt, Germany). N<sub>2</sub> gas was obtained from Linde gas (Turkey). Millipore Milli-Q Advantage A10 apparatus (Darmstadt, Germany) was used to produce 18 MΩ.cm (25 °C) ultra-pure water. Experiments were performed in BERGHOF BR-100 high-pressure reactor equipped with BLH-800 heating plate with built-in magnetic stirrer (Eningen, Germany). This reaction system is resistant to high pressure and provides safer working compared to the one used in the previous study [40]. COD cell kits with measurement range of 0–150 mg/L were provided from Hach Lange (Düsseldorf, Germany). COD values of samples were measured using WTW Photolab 6100 Vis Spectrophotometer (Shimadzu UV-1601). Chebios Optimum-One (Rome, Italy) UV–Vis spectrophotometer was used to measure the concentration of the samples. Perkin Elmer Spectrum-100 (Beaconsfield, England) was used to record FT-IR spectra of the samples. Bruker Ultrashield Plus Biospin Avance III 400 MHz NaNoBay FT-NMR was employed to record NMR spectra. Heidolph Hei-VAP rotary evaporator (Schwabach, Germany) was used for the evaporation of the samples.

### Degradation method

150 mL of initial 2-NA solution (100 ppm) was subjected to degradation in each experiment. CCD method was employed to assign treatment conditions such as temperature, treatment time, and the oxidising agent at three levels, as demonstrated in Table 1. The initial internal pressure of the high-pressure reactor (BERGHOF BR-100) was fixed to 30 bar by using N<sub>2</sub>. Fractions were collected at the end of each experiment for further analysis.

**Table 1** Experimental design of the independent variables used in CCD

Factors	Independent variables	Coded levels				
		$-\alpha$	$-1$	$0$	$1$	$+\alpha$
$x_1$	Temperature (K)	339	373	423	473	507
$x_2$	Treatment time (min)	9.55	30	60	90	110.5
$x_3$	Concentration of oxidising agent (mM)	9.55	30	60	90	110.5

## Analysis methods

### COD analysis

COD removal percentages were determined by COD cell kits. A specific amount of the collected fractions (treated samples) and the initial solution (untreated sample) were spectrometrically analysed and degradation efficiencies were calculated in terms of COD removal percentages (COD, %) by comparing their COD values according to Eq. 1:

$$\text{COD, \%} = [(C_i - C_f)/(C_i)] \times 100. \quad (1)$$

In this formulae,  $C_i$  and  $C_f$  stand for COD values of the initial and treated samples, respectively.

### UV-Vis analysis

To measure removal percentages of 2-NA in treated samples, concentration values of 2-NA were measured by UV-Vis spectrophotometer at wavelengths of 301 and 417 nm, respectively. The removal percentages of treated samples were determined using calibration curves with  $R^2$  values of 0.9986 and 0.9963, respectively. These curves are constituted using UV absorbances of a series of standard solutions in the working range against their concentrations for both wavelengths mentioned above.

### FT-IR and NMR analyses

FT-IR and NMR analyses were performed to identify the remained functional groups (such as  $\text{NO}_2$  and  $\text{NH}_2$ ) in the treated samples and their degradation rate as well as to interpret the degradation of 2-NA. Treated samples were extracted with ethyl acetate, filtered through Whatman filter paper 4 and dried over  $\text{Na}_2\text{SO}_4$ . Finally, the organic phase was evaporated using a rotary evaporator. FT-IR spectra were recorded by Perkin Elmer Spectrum-100 between 4000 and  $650 \text{ cm}^{-1}$  at room temperature using obtained solid specimen.  $^{13}\text{C}$ -NMR and  $^1\text{H}$ -NMR spectra were recorded using the  $\text{CDCl}_3$  solution of the mentioned solid.

## CCD modeling

RSM is a useful collection of statistical and mathematical techniques to optimise and model the processes [32, 33, 43]. It provides a variety of sophisticated models to reduce workload and cost, to evaluate the relationship between operating parameters and response, and to establish approximation equations. CCD is the most preferred one of these models. This method is used to build a full or fractional factorial second-order RSM model consisting of three types of points in the experimental region [32, 44]. The number of the experiments required in the CCD is given by  $N = 2^k + 2k + C_0$ , where  $k$  stands for the number of the variables and  $C_0$  is the replicate number of central points [33].

Appropriate ranges of the most influential experimental variables such as temperature (K),  $x_1$ , treatment time (min),  $x_2$ , and concentration of  $\text{H}_2\text{O}_2$  (mM),  $x_3$ , as the oxidising agent were determined according to preliminary experiments and literature review. The effect of these three variables on the dependent variable, COD removal percentage, was investigated in subcritical water medium using  $\text{H}_2\text{O}_2$  at five levels according to CCD, as demonstrated in Table 1.

The experimental results were analysed by Design Expert 9.0.6.2 version and the regression model was suggested. Results of 20 experiments, namely, experimental COD removal percentage of all runs, are depicted in Table 2 along with predicted values.

The correlation of response and independent variables was represented using linear or quadratic models (Eq. 2):

$$Y = \beta_0 + \beta_1 x_1 + \beta_2 x_2 + \beta_3 x_3 + \beta_{12} x_1 x_2 + \beta_{13} x_1 x_3 + \beta_{23} x_2 x_3 + \beta_{11} x_1^2 + \beta_{22} x_2^2 + \beta_{33} x_3^2 + \epsilon. \quad (2)$$

In this equation,  $Y$  depicts the response,  $x_1$ ,  $x_2$ , and  $x_3$  symbolize the coded independent variable effects, and  $x_1^2$ ,  $x_2^2$ , and  $x_3^2$  represent the quadratic effects.  $x_1 x_2$ ,  $x_1 x_3$ , and  $x_2 x_3$  demonstrate interaction effects.  $\beta_1$ ,  $\beta_2$ , and  $\beta_3$  are the linear coefficients, and  $\beta_{11}$ ,  $\beta_{22}$ ,  $\beta_{33}$  are the quadratic coefficients.  $\beta_{12}$ ,  $\beta_{13}$ , and  $\beta_{23}$  are the interaction coefficients.  $\beta_0$  and  $\epsilon$  represent the constant and the random error, respectively [32, 34, 45]. ANOVA was performed to statistically evaluate the employed quadratic model and its terms. In addition,

**Table 2** Experimental results of COD removal percentages and predicted values obtained by CCD and ANN

Run	Temperature (K)	Treatment time (min)	Concentration of oxidising agent (M)	COD removal, %			AD <sub>1</sub>	AD <sub>2</sub>
				Exp.	CCD Pre.	ANN Pre.		
1	423 (0)	9.55 (− 1.682)	60 (0)	72.22	73.04	72.41	0.82	0.19
2	423 (0)	60 (0)	60 (0)	72.84	75.80	77.55	2.96	4.71
3	423 (0)	60 (0)	110.5 (+ 1.682)	67.90	69.91	65.08	2.01	2.82
4	473 (+ 1)	30 (− 1)	30 (− 1)	78.52	80.15	78.03	1.63	0.49
5	373 (− 1)	90 (+ 1)	30 (− 1)	60.49	59.68	60.79	0.81	0.30
6	339 (− 1.682)	60 (0)	60 (0)	40.99	44.70	41.34	3.71	0.35
7	373 (− 1)	30 (− 1)	30 (− 1)	51.23	49.21	51.45	2.02	0.22
8	473 (+ 1)	30 (− 1)	90 (+ 1)	77.61	77.02	77.03	0.59	0.58
9	423 (0)	110.5 (+ 1.682)	60 (0)	71.99	73.14	72.47	1.15	0.48
10	423 (0)	60 (0)	9.55 (− 1.682)	70.37	70.33	70.94	0.04	0.57
11	373 (− 1)	30 (− 1)	90 (+ 1)	63.37	61.84	62.04	1.53	1.33
12	507 (+ 1.682)	60 (0)	60 (0)	76.12	74.38	75.94	1.74	0.18
13	423 (0)	60 (0)	60 (0)	80.42	75.80	77.55	4.62	2.87
14	473 (+ 1)	90 (+ 1)	90 (+ 1)	66.05	66.67	66.14	0.62	0.09
15	423 (0)	60 (0)	60 (0)	72.84	75.80	77.55	2.96	4.71
16	423 (0)	60 (0)	60 (0)	74.69	75.8	77.55	1.11	2.86
17	473 (+ 1)	90 (+ 1)	30 (− 1)	79.67	79.8	79.97	0.13	0.30
18	423 (0)	60 (0)	60 (0)	77.78	75.8	77.55	1.98	0.23
19	423 (0)	60 (0)	60 (0)	76.54	75.8	76.58	0.74	0.04
20	373 (− 1)	90 (+ 1)	90 (+ 1)	65.33	62.31	65.24	3.02	0.09

AD<sub>1</sub> absolute difference between experimental values and CCD predicted values, AD<sub>2</sub> absolute difference between experimental values and ANN predicted values

the adequacy of the model was assessed by regression coefficients, ( $R^2$ ,  $R^2_{adj}$ ), Fisher's 'F' test, and P values.

### ANN modeling

The basis of ANN is established on the predicting the non-linear relationship between independent variables (input layers) such as  $x_1$ ,  $x_2$ , and  $x_3$ , and response variables, Y [40, 41]. ANN determines this relationship by the biological neural network model which generated from the idea of the mechanical function of the human brain [46, 47]. ANN does not require prior patterns to learn the interaction between interested samples [40–42]. This feature of the ANN makes it the unique model in the solution of complex problems in various applications [46].

A feed-forward back propagation ANN model, based on multilayer perceptron (MLP), composed of input, hidden, and output layers was applied in the non-linear analysis of mineralisation of 2-NA. Many ANN architectures composed of a various number of layers and nodes (neurons) in each layer and several transfer functions and learning algorithms were tested to achieve the best ANN model in the desired level of precision. The optimal three-layer feed forward ANN model is depicted in Fig. 1. As shown from this figure, the input layer consists of three neurons which

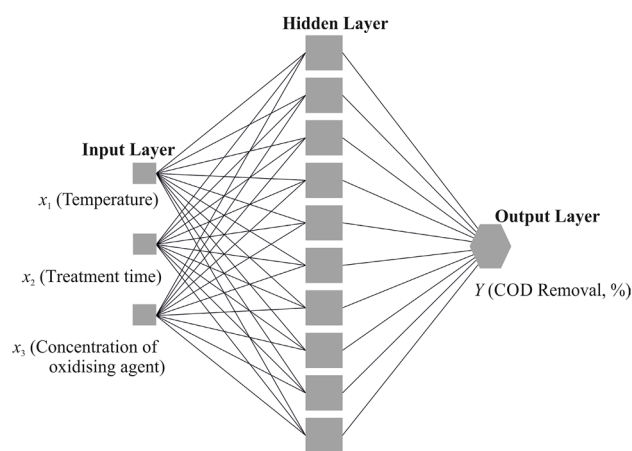


**Fig. 1** Optimal structure of three-layer feed forward ANN model

represent three experimental variables, namely,  $x_1$ ,  $x_2$ , and  $x_3$ . In addition, only one hidden layer with 10 neurons was chosen in this study, because more hidden layers may lead to over-fitting problems [41]. An output layer that symbolizes the response (COD removal, %) was represented by one neuron.

The experimental data which are given in Table 2 were used to build an ANN model as utilized for CCD. Randomly

selected 14 points (70% of all runs), 3 points (15% of all runs), and 3 points (15% of all runs) were utilized for training the network, for validation, and for testing the network, respectively. The Neural Network Toolbox of MATLAB software (R2015a ver. 8.6, The Mathworks, Inc., Massachusetts, USA) was employed for ANN modeling.

## Results and discussion

The values of the independent process variables and experimental COD removal rates are given in Table 2. In addition, Table 2 shows predicted values of COD removal percentages that are obtained by CCD and ANN modeling. The interactions between system variables and the response can be simply demonstrated using RSM. The highest experimental COD removal percentages were achieved at run 13, one of the 6 center point of the CCD design model, as 80.42%. The predicted values of COD removal percentages of this run were obtained as 75.80 and 77.55%, employing CCD and ANN, respectively. The lowest experimental COD removal rate was achieved at run 6, which was performed at the lowest temperature of the design, as 40.89%. CCD and ANN predicted the COD removal rates for run 6 as 44.70 and 41.34%, respectively.

### Evaluation of the optimisation using CCD modeling

Experimental data, which are demonstrated in Table 2, were used to fit the second-order polynomial equation, as given in Eq. 3. The response of the process, namely, COD removal percentage, can be simply associated to independent variables using this equation. In addition, Eq. 3 can be used to predict the response under different conditions and to evaluate the interaction between all variables:

$$Y_1 = 8.82x_1 + 0.031x_2 - 0.12x_3 - 2.70x_1x_2 - 3.94x_1x_3 - 2.50x_2x_3 - 5.75x_1^2 - 0.96x_2^2 - 2.01x_3^2 + 75.80. \quad (3)$$

In addition, the effects of the variables can be clearly seen in Fig. 2, which provides a comparison of the coefficient of the model terms. This figure demonstrates a graphical analysis of the effects of the variables, including positive, negative, quadratic, and interactive effects, on the investigated COD removal rates of 2-NA. Figure 2 shows that the most effective variable for the COD removal of 2-NA is temperature,  $x_1$ , where its quadratic effect  $x_1^2$ , is the second most effective variable that inversely affects the response. Nevertheless, the rank of interactive effects of the variables is  $x_1x_3 > x_1x_2 > x_2x_3$ . Treatment time,  $x_3$ , and concentration of the oxidising agent,  $x_2$ , are very ineffective factors on the COD removal of 2-NA.

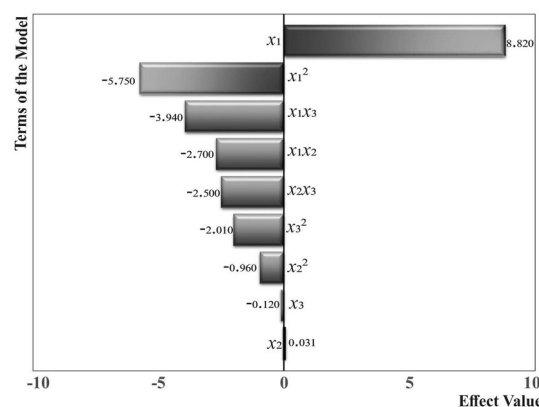


Fig. 2 Graphical analysis of the effect of the CCD model

The evaluation of the fit of the experimental data was performed by ANOVA analysis. Table 3 demonstrates ANOVA results of the quadratic model obtained for COD removal rates of 2-NA. It can be said, according to ANOVA terms, that  $F$  and  $p$  values of the model were obtained at an appropriate value. Thus, the values of  $F$  and  $p$  were obtained as 23.03 and lower than 0.0001, respectively, which indicates that the model is statistically significant. There is only a 0.01% chance that an  $F$  value this large could occur due to noise. In addition, considering that a value of  $p$  lower than 0.05 is reasonable [32], it is clear that  $x_1x_3 > x_1x_2 > x_2x_3$ ,  $x_1^2$ , and  $x_3^2$  are the other significant terms of the investigated model.

### Regression and correlation analysis of CCD model

The reliability of a quadratic model employed in this study, obtained by CCD, was evaluated in terms of regression and correlation analysis. The obtained coefficients and other values are tabulated in Table 4. The predicted residual sum of squares (PRESS) value can measure the level of model fit to each point in the design [32]. According to this definition, it can be said that the employed model adapts to every point and the reasonable difference was obtained between actual and predicted values over PRESS value of 391.70.

In addition, the  $R^2$  value, which is an indication of model conformity and is described between zero and one, was found to be 0.9540 for the CCD model. Thus, it can be said that the obtained model is significant over the  $R^2$  value that high value was obtained. Furthermore, adjusted  $R^2$  and predicted  $R^2$ , which indicate the amount of variation around the mean presented by the employed model and variation in the new data explained by the used model, were found as 0.9126 and 0.7928, respectively [32]. These values are in a quite close proximity, where closeness is desired to claim the determination of a high correlation level between experimental and predicted results of the employed model.



**Table 3** ANOVA results of quadratic model obtained by CCD

Source	Sum of squares	df	Mean square	F value	p value prob > F
Model	1803.17	9	200.35	23.03	<0.0001
$x_1$	1063.42	1	1063.42	122.26	<0.0001
$x_2$	0.013	1	0.013	$1.508 \times 10^{-3}$	0.9698
$x_3$	0.21	1	0.21	0.024	0.8789
$x_1x_2$	58.48	1	58.48	6.72	0.0268
$x_1x_3$	124.11	1	124.11	14.27	0.0036
$x_2x_3$	50.05	1	50.05	5.75	0.0374
$x_1^2$	475.93	1	475.93	54.72	<0.0001
$x_2^2$	13.17	1	13.17	1.51	0.2466
$x_3^2$	58.00	1	58.00	6.67	<0.0273
Residual	86.98	10	8.70		
Lack of fit	42.43	5	8.49	0.95	0.5207
Pure error	44.45	5	8.91		
Cor. total	1890.15	19			

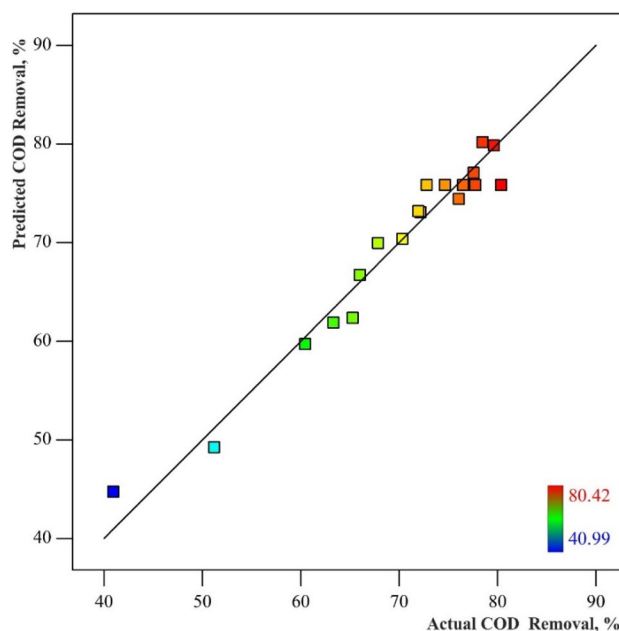
**Table 4** Regression and correlation analyses of the obtained models by CCD

Regression coefficients			
<b>Standard deviation</b>	2.95	<b>R<sup>2</sup></b>	0.9540
<b>Mean</b>	69.85		0.9126
<b>C.V. %</b>	4.22	<b>Predicted R<sup>2</sup></b>	0.7928
<b>Press</b>	391.70	<b>Adequate precision</b>	16.997

2.95 value of standard deviation, which is also known as the square root of the residual mean square, is satisfactory, where low value is desired. C.V. % (Coefficient of variation) value, which is calculated by dividing the standard deviation by the mean and multiplying by 100, was found to be 4.22. A measure of the signal-to-noise ratio is expressed by the adequate precision value which is used in the comparison of the range of the predicted values and the design points to the average prediction error [30]. While the sufficient adequate precision value has to be higher than 4 to verify the utilization of the model in the navigation of the design space, the mentioned value was found to be 16.997 in the performed CCD model [30, 32].

The relation between the actual and predicted values of COD removal rates of 2-NA is displayed in Fig. 3. The compatibility within the points which represent the actual and predicted values can be clearly seen from this figure. This compatibility was also stated above by showing the accordance within  $R^2$  and adjusted  $R^2$  and predicted  $R^2$ .

Figure 4 displays the plot of the CCD model for COD removal rates of 2-NA. The predicted values of COD removal percentage from the coded model for the combination of the  $-1$  and  $+1$  levels of any three independent variables are demonstrated in this figure. In addition, Fig. 4 facilitates the evaluation of data composed of three independent

**Fig. 3** Relation between the actual and predicted values of COD removal rates of 2-NA

factors with the highest and the lowest value of them. In addition, further predictions in the experimental region and required conditions can be displayed by the aid of Fig. 4.

### Evaluation of binary effects of the process variables on the mineralisation rates

Three-dimensional (3D) response surface plots were demonstrated to evaluate the binary effects of variables on the COD removal percentages of 2-NA. Thus, the observation

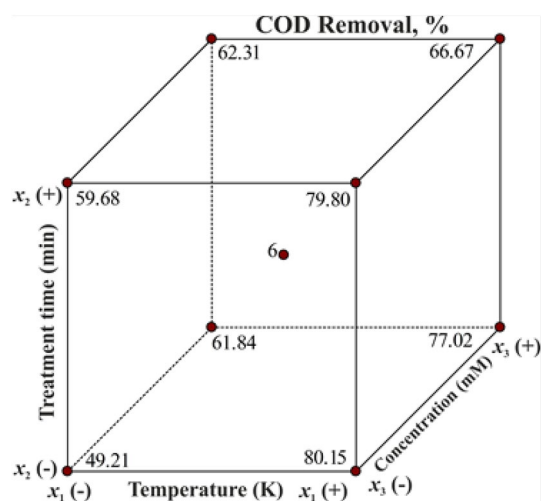


Fig. 4 Cube plot of the CCD model for COD removal rates of 2-NA

of the interactive effects of experimental variables on the response provides the evaluation of the response effectively.

The 3D plot of binary effects of oxidant concentration and treatment time on the COD removal percentages of 2-NA at a fixed temperature of 473 K is demonstrated in Fig. 5. As clearly seen from Fig. 5, the interaction effect of  $\text{H}_2\text{O}_2$  concentration and treatment time is crucial on the COD removal rates of 2-NA at 473 K of temperature. However, when the conditions in Fig. 5 were kept the same, the decrease in the

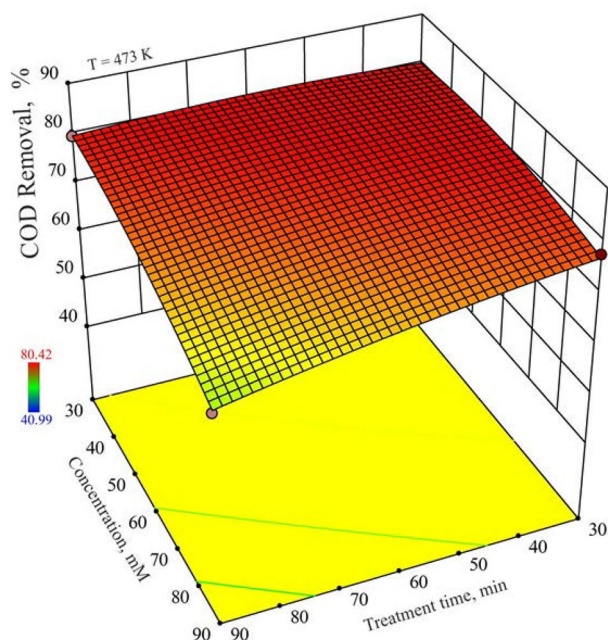


Fig. 5 Binary effects of oxidant concentration (C) and treatment time (min) on the COD removal percentages of 2-NA at the fixed temperature of 473 K

COD removal rates was observed by lowering the temperature from 473 to 423 and 373 K, respectively. Moreover, it was observed that there is no significant effect on the efficiency to change treatment time and oxidant concentration below the moderate temperatures. However, it was observed that the concentration of  $\text{H}_2\text{O}_2$  and the treatment time has a positive effect to a certain extent at high temperature, while higher concentration and treatment time decrease the efficiency. For instance, while COD removal percentages of 2-NA were observed from the CCD model as 80.93% at 30 mM of concentration of  $\text{H}_2\text{O}_2$ , and 60 min of treatment time, it was observed that COD removal decreased to 67.05% at 90 mM of concentration of  $\text{H}_2\text{O}_2$ , and 90 min of treatment time when keeping the temperature of reaction medium at fixed 473 K of temperature. This decline can be explained by the fact that, above a certain effective concentration of  $\text{H}_2\text{O}_2$ , some of them transform into active radicals and enter into chain reactions among themselves rather than attacking and degrading 2-NA [30, 48]. It is also seen that increasing the treatment time in the presence of the high concentration of  $\text{H}_2\text{O}_2$  at 473 K has a limited effect on COD removal efficiency.

Figure 6 demonstrates the interactive effect of treatment time and temperature on COD removal percentages of 2-NA at fixed oxidant concentration of 30 mM. The COD removal rate was found to be reasonably depend on the interaction of treatment time and temperature. Thus, when fixing the concentration of  $\text{H}_2\text{O}_2$  at 90 mM, elevated COD removal efficiency was obtained even at short treatment time, but at high

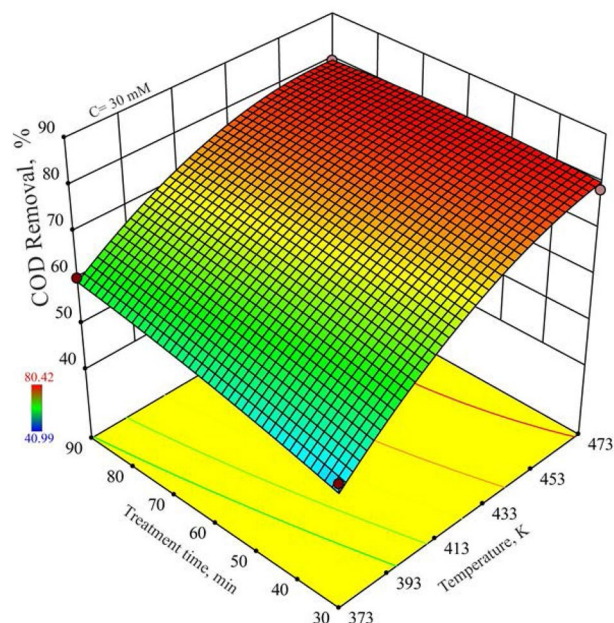
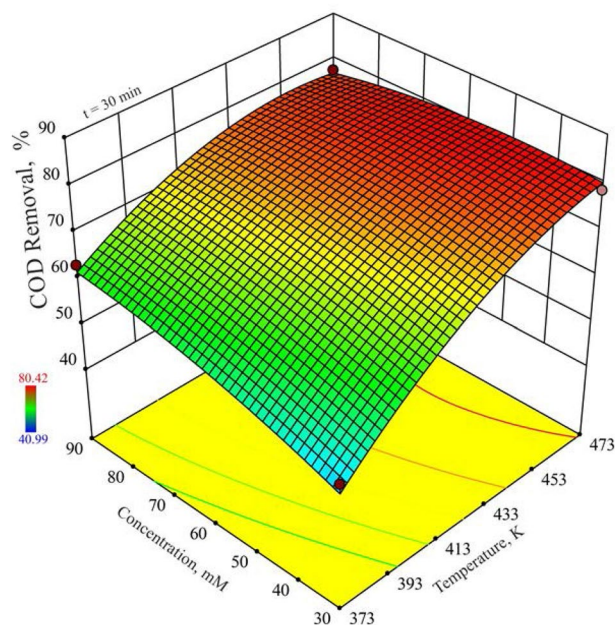


Fig. 6 Binary effects of treatment time (min) and temperature (T) on the COD removal percentages of 2-NA at the fixed oxidant concentration of 30 mM

temperatures. However, the interaction effect of treatment time and temperature on the efficiency tends to increase at medium levels of temperature and treatment time when fixing the concentration of  $\text{H}_2\text{O}_2$  at 60 mM. Furthermore, high COD removal rates were obtained at all levels of treatment time, above moderate temperatures and at a fixed  $\text{H}_2\text{O}_2$  concentration of 30 mM. For instance, 79.35% of COD removal was found to decrease to 79.31 and 77.35%, respectively, at 433 K of temperature and 30 mM of the oxidising agent when decreasing the treatment time from 90 min to 60 and 30 min, respectively. These findings support the fact that subcritical water oxidation method using  $\text{H}_2\text{O}_2$  is a superior alternative to traditional methods, considering obtainable high efficiency even in the short treatment time and reasonable concentration level of oxidising agent.

Figure 7 displays binary effects of oxidant concentration and temperature on the COD removal percentages of 2-NA at the fixed treatment time of 30 min. High temperature activates  $\text{H}_2\text{O}_2$  to convert it into radical species and leads to effective degradation of the target molecule. However, though lower temperatures are sufficient to activate  $\text{H}_2\text{O}_2$ , the application of relatively higher temperatures for the mineralisation of 2-NA may be attributed to its degradation-resistant structure, similar to the structure of many other nitroaromatic compounds [28, 49]. In addition, there is no need to increase the concentration of  $\text{H}_2\text{O}_2$  in conditions, in which the low or high oxidant concentration values above the moderate temperatures during the 30 min of treatment time do not make a significant difference in COD removal efficiency. It was obtained that COD removal



**Fig. 7** Binary effects of oxidant concentration (C) and temperature (T) on the COD removal percentages of 2-NA at the fixed treatment time of 30 min

was only increased from 75.15 to 77.14% when increasing  $\text{H}_2\text{O}_2$  concentration from 30 to 90 mM at 433 K of temperature and 30 min of treatment time. However, when the treatment time is increased to 90 min, the graphical area presenting high yield is sharply reduced and even  $\text{H}_2\text{O}_2$  concentration has a negative effect on the yield under these conditions.

### ANN modeling and comparison between CCD and ANN

ANN modeling was applied for the estimation of COD removal rates of 2-NA and obtained results of the predicted values of both models are given in Table 2. The lowest and the highest COD removal percentages which were obtained as 41.34% and 79.97%, respectively, in the run of 6 and 17, respectively, were found to be very close to the experimental value of each one, as demonstrated in Table 2. In addition, ANN predicted closer values to the experimental values at the center points of experimental runs than CCD. Thus, ANN showed better performance in these cases when comparing to CCD. Absolute differences between experimental values and ANN predicted values ( $AD_2$ ) were found to be higher than the absolute differences between experimental values and CCD predicted values ( $AD_1$ ) at factorial point such as run 17, at center points such as run 2, 15, and 16 at axial points such as run 3 and 10, whereas  $AD_1$  values were found to be higher than  $AD_2$  values in the all other points.  $AD_1$  and  $AD_2$  values were found to be quite close to each other at run8 and 17. Moreover,  $AD_2$  values were prominent at the center points, whereas remarkable  $AD_1$  values were obtained at the large part of the central points, following by axial and factorial points. These findings demonstrate that ANN provides a better accordance between predicted and experimental values.

In addition, comparison between the capabilities of ANN and CCD models in the optimisation and prediction of COD removal rates of 2-NA was exhibited by  $R^2$ , RMSE, and AAD values, as given in Table 5. When considering the comparison between the values obtained by ANN model with the values obtained by the CCD model, it is seen that ANN is more superior than CCD model due to predicting closer values to the experimental values. Furthermore,  $R^2$  and RMSE values, which mean that the predicted values match with experimental values, supported this phenomenon. In other words, while AAD values were lower for CCD than for ANN, RMSE values were found to be 1.90 and 2.09, respectively, for ANN and CCD, where a lower value of RMSE indicates the best

**Table 5** Comparison between the performance of ANN and CCD models for prediction of COD removal rates of 2-NA

Source	CCD	ANN
$R^2$	0.9540	0.9643
RMSE	2.09	1.90
AAD	7.47	7.90



### Evaluation of UV-Vis Analysis

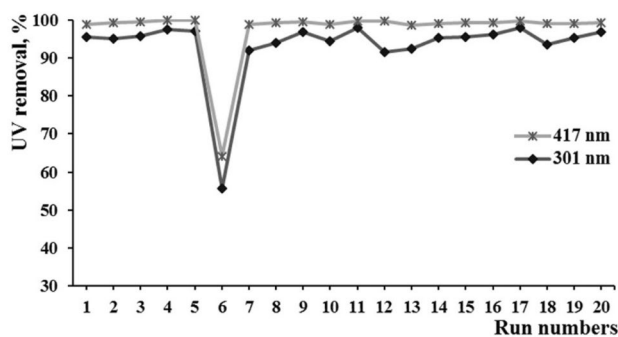


**Fig. 8** Removal rates of 2-NA at 301 nm and 417 nm

performance of the model [41, 43]. In addition, the  $R^2$  values were found to be 0.9643 and 0.9547, respectively, for ANN and CCD, where the higher of  $R^2$  shows the better data fitting performance [41, 43].

### Evaluation of UV-Vis analysis

Figure 8 demonstrates the UV-Vis analysis results of the experimental runs done under the conditions, as given in Table 2. While COD removal is crucial in determining the rate of mineralisation, UV-Vis data are also important in determining the removal rates of 2-NA. According to UV-Vis analysis, the removal of 2-NA was obtained as 55.61% at 301 nm and 64.12% at 417 nm for Run 6. Although these values are higher compared to the COD removal, it is relatively low compared to other removal percentages of 2-NA. The low level of the removal rate of run 6 can be attributed to the presence of low  $H_2O_2$  concentration in the reaction medium and low temperature, which may limit the formation of effective free radicals and the removal of 2-NA. Removal rates of other runs, except run 6, were obtained in the ranges of 91.60–97.95% at 301 nm, and 98.66–99.88% at 417 nm. It has been shown that the 2-NA was efficiently removed from the aquatic environment based on the removal results. Thus, the efficacy of the subcritical water degradation method using  $H_2O_2$  is also demonstrated by the removal results obtained by UV-Vis data.

### Evaluation of FT-IR and NMR analyses

COD and UV-Vis results were also supported by FT-IR and NMR analyses of the extracts obtained after extraction of the treated samples with EtOAc. The FT-IR and NMR spectra for untreated 2-NA and treated 2-NA samples were compared, respectively (this section was given in the Supplementary material).

### Conclusion

The mineralisation of 2-nitroaniline from the artificially contaminated water solution was achieved using the simple, effective, and eco-friendly subcritical water degradation method with the powerful oxidising agent,  $H_2O_2$ . The mineralisation rates were monitored by COD removal analysis. To determine the effects of all employed variables, namely, temperature, concentration of oxidising agent and treatment time, on the COD removal rates and interactions between themselves, CCD modeling in RSM was applied in this work. Optimum conditions for elevated mineralisation of 2-NA were determined and ANOVA and mathematical equations were provided for the applied CCD model of COD removal. While all chosen parameters were found to influence the mineralisation rate, temperature was proved to be the most effective one. 80.43% of COD removal was obtained under optimum mineralisation conditions, which were determined using CCD modeling, at 463 K of temperature, 53.4 mM of  $H_2O_2$  concentration and 32 min of treatment time. In addition, the most preferred CCD and ANN models were used for prediction of the COD removal rates for further evaluations and their efficiencies were compared by  $R^2$ , RMSE and AAD values. The obtained results revealed that the ANN model is a superior method than CCD, predicting the closer values of COD removal rates to the experimental value than the values predicted by CCD. The removal rate, which was measured by UV-Vis spectrometric analysis, is an important parameter in the purification of waters due to showing how much of the contaminant is removed. Thus, removal of 2-NA was also analysed by measuring UV absorbances of treated samples. In addition, the degradation process is followed by FT-IR and NMR analyses by comparing the FT-IR and NMR spectra of untreated and treated samples, respectively. Thus, the degradation of the groups in the 2-NA structure was followed to support the mineralization and removal values revealed by COD and removal rates, and the effectiveness of subcritical water oxidation for the mineralisation of 2-NA was demonstrated.

**Acknowledgements** This academic work was linguistically supported by the Mersin Technology Transfer Office Academic Writing Center of Mersin University.

### References

1. A.G. Karunanayake, O.A. Todd, M.L. Crowley, L.B. Ricchetti, C.U. Pittman, R. Anderson, T.E. Mlsn, *Chem. Eng. J.* **319**, 75 (2017)
2. T. Heberer, *Toxicol. Lett.* **131**, 5 (2002)
3. T. Rastogi, C. Leder, K. Kuemmerer, *Environ. Sci. Technol.* **49**, 11756 (2015)

4. G. Kinrys, A.K. Gold, J.J. Worthington, A.A. Nierenberg, J. Int. Med. Res. **46**, 927 (2018)
5. B. Du, A.E. Price, W.C. Scott, L.A. Kristofco, A.J. Ramirez, C.K. Chambliss, J.C. Yelderman, B.W. Brooks, Sci. Total Environ. **466–467**, 976 (2014)
6. A. Qureshi, V. Verma, A. Kapley, H.J. Purohit, Int. Biodeterior. Biodegrad. **60**, 215 (2007)
7. N. Mark, J. Arthur, K. Dontsova, M. Brusseau, S. Taylor, Chemosphere **144**, 1249 (2016)
8. K.O. Garcia, E.C. Teixeira, D.M. Agudelo-Castañeda, M. Braga, P.G. Alabarse, F. Wiegand, Sci. Total Environ. **479–480**, 57 (2014)
9. C.L. He, K.L. Huang, J.H. Huang, J. Colloid Interface Sci. **342**, 462 (2010)
10. M.E. Mahmoud, A.E.H. Abdou, A.K. Shehata, H.M. Header, E.A. Hamed, J. Mol. Liq. **224**, 1358 (2016)
11. O.A. Zelekew, D.H. Kuo, Appl. Surf. Sci. **393**, 110 (2017)
12. P. Guo, L. Tang, J. Tang, G. Zeng, B. Huang, H. Dong, Y. Zhang, Y. Zhou, Y. Deng, L. Ma, S. Tan, J. Colloid Interface Sci. **469**, 78 (2016)
13. K.Q. Li, Y. Li, Z. Zheng, J. Hazard. Mater. **178**, 553 (2010)
14. Z.H. Farooqi, K. Naseem, R. Begum, A. Ijaz, J. Inorg. Organomet. Polym. Mater. **25**, 1554 (2015)
15. K. Li, Z. Zheng, X. Huang, G. Zhao, J. Feng, J. Zhang, J. Hazard. Mater. **166**, 213 (2009)
16. Z. Dong, X. Le, X. Li, W. Zhang, C. Dong, J. Ma, Appl. Catal. B **158–159**, 129 (2014)
17. P. Yang, A.D. Xu, J. Xia, J. He, H.L. Xing, X.M. Zhang, S.Y. Wei, N.N. Wang, Appl. Catal. A **470**, 89 (2014)
18. S. Silambarasana, A.S. Vangnaia, J. Hazard. Mater. **302**, 426 (2016)
19. Y. Wang, Y. Zhang, G. Zhao, M. Wu, M. Li, D. Li, Y. Zhang, Y. Zhang, Sep. Purif. Technol. **104**, 229 (2013)
20. Y.S. Zhao, C. Sun, J.Q. Sun, R. Zhou, Sep. Purif. Technol. **142**, 182 (2015)
21. J.H. Sun, S.P. Sun, M.H. Fan, H.Q. Guo, Y.F. Lee, R.X. Sun, J. Hazard. Mater. **153**, 187 (2008)
22. L. Ding, Q. Li, D. Zhou, H. Cui, R. Tang, J. Zhai, Electrochim. Acta **77**, 302 (2012)
23. A. Khalid, M. Arshad, D.E. Crowley, Water Res. **43**, 1110 (2009)
24. S. Gautam, S.P. Kamble, S.B. Sawant, V.G. Pangarkar, Chem. Eng. J. **110**, 129 (2005)
25. J. Zhang, D. Shan, S. Mu, Polymer **48**, 1269 (2007)
26. J. Zhang, D. Shan, S. Mu, J. Polym. Sci. A Polym. Chem. **45**, 5573 (2007)
27. N. Wang, T. Zheng, J. Jiang, P. Wang, Chem. Eng. J. **260**, 386 (2015)
28. H.H. Sun, S.P. Sun, M.H. Fan, H.Q. Guo, L.P. Qiao, R.X. Sun, J. Hazard. Mater. **148**, 172 (2007)
29. J. Levec, A. Pintar, Catal. Today **124**, 172 (2007)
30. E. Yabalak, H.A. Döndaş, A.M. Gizir, J. Environ. Sci. Heal. A **52**, 210 (2017)
31. E. Yabalak, A.M. Gizir, J. Serb. Chem. Soc. **78**, 1013 (2013)
32. E. Yabalak, A.S. Könen, A. Adigüzel, R.S. Ergene, M. Tunçer, A.M. Gizir, Desalin. Water Treat. **81**, 186 (2017)
33. E. Yabalak, Ö Görmez, B.G. Sönmez, J. Serb. Chem. Soc. **83**, 489 (2018)
34. R.S. Ribeiro, A.M.T. Silva, J.L. Figueiredo, J.L. Faria, H.T. Gomes, Appl. Catal. B-Environ. **187**, 428 (2016)
35. P.R. Gogate, A.B. Pandit, Adv. Environ. Res. **8**, 501 (2004)
36. S. Daneshvar, N. Hidemi, F. Salak, N. Mahinpey, Can. J. Chem. Eng. **92**, 615 (2014)
37. E. Yabalak, Ö Görmez, B. Gözmen, A.M. Gizir, Int. J. Ind. Chem. **6**, 23 (2015)
38. N.C. Loong, M. Basri, L.F. Fang, H.R.F. Masoumi, M. Tripathy, R.A. Karjiban, E. Abdul-Malek, Ind. Crops Prod. **59**, 309 (2014)
39. J. Zolgharnein, A. Shahmoradi, J.B. Ghasemi, J. Chemometr. **27**, 12 (2013)
40. E. Yabalak, J. Environ. Sci. Health, Part A (2018) <https://doi.org/10.1080/10934529.2018.1471023>
41. J.A. Lin, C.Hng Kuo, B.Y. Chen, Y. Li, Y.C. Liu, J.H. Chen, C.J. Shieh, Ultrason. Sonochem. **32**, 258 (2016)
42. K.M. Desai, S.A. Survase, P.S. Saudagar, S. Lele, R.S. Singhal, Biochem. Eng. J. **41**, 266 (2008)
43. K. Ameer, S.W. Bae, Y. Jo, H.G. Lee, A. Ameer, J.H. Kwon, Food Chem. **229**, 198 (2017)
44. C.R.T. Tarley, G. Silveira, W.N.L. dos Santos, G.D. Matos, E.G.P. da Silva, M.A. Bezerra, M. Miró, S.L.C. Ferreira, Microchem. J. **92**, 58 (2009)
45. Z. Zhang, H. Zheng, J. Hazard. Mater. **172**, 1388 (2009)
46. H. Okuyucu, A. Kurt, E. Arcaklioglu, Mater. Des. **28**, 78 (2007)
47. K.L. Hsu, H.V. Gupta, S. Sorooshian, Water. Resour. Res. **31**, 2517 (1995)
48. B. Kayan, B. Gözmen, J. Hazard. Mater. **201–202**, 100 (2012)
49. N.E. Jiménez Jado, C. Fernández Sánchez, J.R. Ochoa, Gómez, J. Appl. Electrochem. **34**, 551 (2004)